

Numerical study of ferromagnetic fluctuations and pairing correlations in the single-band Hubbard model on the triangular lattice

Shi-Quan Su,¹ Zhong-Bing Huang,² Rui Fan,¹ and Hai-Qing Lin¹

¹*Department of Physics and Institute of Theoretical Physics, The Chinese University of Hong Kong, Hong Kong, China*

²*Faculty of Physics and Electronic Technology, Hubei University, Wuhan 430062, People's Republic of China*

(Received 23 July 2007; revised manuscript received 18 February 2008; published 12 March 2008)

We perform a numerical study using both determinantal and constrain path Monte Carlo methods to investigate the magnetic and pairing properties of the single-band Hubbard model on the triangular lattice. We find that the system in the filling region $\langle n \rangle = 1.5 - 1.85$ shows a short-ranged ferromagnetic correlation, and the on-site Coulomb interaction tends to strengthen ferromagnetic fluctuation slightly. It is shown that the large density of states near the Van Hove singularity point plays an important role in the enhancement of ferromagnetic fluctuation. In the ferromagnetic region, we observe that the f -wave pairing correlation tends to increase faster than other pairing correlations. However, it is subtle to stabilize the f -wave pairing since the effective pairing interaction was found to be very small.

DOI: [10.1103/PhysRevB.77.125114](https://doi.org/10.1103/PhysRevB.77.125114)

PACS number(s): 71.10.Fd, 71.27.+a, 74.20.Rp, 75.40.Mg

I. INTRODUCTION

Recently, there has been a growing interest in studying the correlated electron system on frustrated lattices such as a two-dimensional triangular lattice.^{1,2} This was stimulated by the discovery of $\text{Na}_x\text{CoO}_2 \cdot y\text{H}_2\text{O}$ (Ref. 3) and organic conductors such as $\theta\text{-(DIETS)}_2[\text{Au}(\text{CN})_4]$,⁴ which show interesting magnetic, charge, and superconductivity properties. The one-band Hubbard model, which is the minimal model to describe interacting electrons, has been used to understand the fascinating physical properties of low-dimensional correlated electron systems.⁵⁻⁷ Most of them have been extensively studied but not all are well understood. Among them, one of an old and still unclear issues concerns the ferromagnetic property of itinerant electrons. After extensive studies of the Hubbard model and its extended versions, there are still only few rigorous results about ferromagnetic properties. These results mainly include three kinds. The first exact result of the Hubbard model comes from the so-called Nagaoka state.⁸ In the system that has an infinite local repulsion, a single electron above half-filling favors the saturated ferromagnetic ground state for certain lattices. These conclusions have been clarified and improved by extensive studies.⁹⁻¹¹ Second, there exists the so-called Lieb ferromagnetism¹² in multiband systems. A system of half-filled bipartite lattices with different numbers of sublattice sites has a unique ferromagnetic-type ground state. These two kinds of ferromagnetism are applicable to the system containing full-filled energy bands without the itinerant electron, which is usually viewed as an insulator. The third one was proposed by Mielke^{13,14} and Tasaki,^{15,16} arguing that a system with nearly flat and partially filled band has a global stable ferromagnetic ground state, if there is no single spin-flip ground state. Since the system contains partially filled bands, it can be interpreted as metallic ferromagnetism. This kind of ferromagnetism may be partially polarized or saturated. There are quite a lot of efforts studying both numerically and analytically devoted to this scenario of metallic ferromagnetism.¹⁷⁻²⁰ It has been known for some times that the geometry of the lattice system, the shape of density of

states (DOS) distribution, and the large degeneracy of single-particle energy level are crucial to the stability of the ferromagnetic state.²¹⁻²³ The triangular lattice, compared to the square lattice, has a higher degeneracy on single-particle energy level and asymmetric distribution of DOS, so it favors stronger ferromagnetic correlation under some situations. The scenario takes place on the triangular lattice having a large DOS region close to the Van Hove singularity point. In this case, if the particle density is high and $U \neq 0$, electrons near the Fermi surface polarized with the same spin may occupy the higher single-particle level according to the Pauli exclusion principle, and the kinetic energy enhancement is not significant because the large DOS makes the width among single-particle levels narrow. On the other hand, the local Coulomb interaction is less active in such a state and the potential energy is reduced. For sufficiently large U , states with total spin $S \neq 0$ may have lower energy than the state with $S = 0$. This may result in a ferromagnetic fluctuation of itinerant (or metallic) nature, as it takes place in a partially filled single band with a finite dispersion. The underlying assumption in this picture is that switch on interaction U does not significantly change the DOS distribution, at least in the region around the Fermi surface.

The pairing correlation behaviors play a very important role in studying superconductivity. On the triangular lattice, a variety of pairing correlation behaviors have been reported in different filling regions with different interactions, and some of them are not conclusive and even contradictive. In the Hubbard model, both d -wave and p -wave superconducting states are stable in the low electron filling region, as suggested by the perturbation theory,^{24,25} but the $d+id$ wave with antiferromagnetic exchange interaction was claimed to be more stable by the renormalization group calculation.²⁶ The low density with disconnected Fermi surface fluctuation exchange calculation suggests a possibility to the f -wave pairing.^{27,28} On the other hand, symmetry-based considerations combined with available experimental data suggest a spin-triplet superconductivity mechanism around the superconducting region, which is near three-quarter filling, as the hexagonal Fermi surface in this case produces a stronger

spin-triplet pairing tendency.²⁹ In the t - J model, usually considered as the strong coupling limit of the Hubbard model, both mean field analysis and variational Monte Carlo studies suggest that $(d+id)$ -wave superconductivity is stable near half-filling.^{1,30,31} The high-temperature expansion calculation suggests that in the high electron density region, a rapid growth of effective d -wave pairing interaction indicates the resonating-valence-bond superconductivity, while in the low-density region, the f -wave pairing dominates, although its effective interaction is small.³²

In this paper, we investigate ferromagnetic fluctuation and the behavior of pairing correlation near the Van Hove singularity point (away from the half-filling) on the triangular lattice. Specifically, we mainly study the electron filling region $1.5 < \langle n \rangle < 1.85$. We study the system in two ways: the grand canonical ensemble at finite temperature and the canonical ensemble at zero temperature. For the grand canonical ensemble, we use the determinant Quantum Monte Carlo method³³ to calculate the spin susceptibility and several kinds of pairing susceptibility (unequal-time correlations in the imaginary-time direction). For the canonical ensemble system, we employ the constrained path Monte Carlo (CPMC) method to compute the ground state energy in different combinations of n_\uparrow , number of spin up particles, and n_\downarrow , number of spin down particles. We also analyze our numerical results under the theoretical frame developed by Mielke¹⁴ and Arrachea²¹ to explore the existence of ferromagnetism.

II. MODEL

The Hamiltonian of the single-band Hubbard model on a triangular lattice reads

$$H = -t \sum_{\langle i,j \rangle, \sigma} (c_{i\sigma}^\dagger c_{j\sigma} + \text{H.c.}) + U \sum_i n_{i\uparrow} n_{i\downarrow} - \mu \sum_{i\sigma} n_{i\sigma}, \quad (1)$$

where $\langle i, j \rangle$ denotes the nearest-neighbor lattice sites i and j , t is the hopping matrix element, U is the on-site repulsive interaction, and μ is the chemical potential. Here, $c_{i\sigma}$ ($c_{i\sigma}^\dagger$) annihilates (creates) a particle with spin σ at site i . The sign of t can be positive or negative, which corresponds to electron and hole picture, respectively. The sign has no physical meaning since both pictures can be related by a particle-hole transformation: $(c_i^\dagger \leftrightarrow d_i)$. In the rest of the paper, we will take $|t|=1$ as the energy unit and $t > 0$, which means that the Hamiltonian describes the electrons' behavior of the system.

As shown in Fig. 1, the model is set on a triangular lattice with hexagonal shape. There are $2N$ sites on the diagonal, and the site number of this series of lattice is $3N^2$. This lattice setting reserves most geometric symmetries of the triangular lattice, and the data points in the first Brillouin zone (BZ) include all the high symmetry points such as Γ , M , and K (shown in the right side of Fig. 1). In the noninteracting case ($U=0$), the band dispersion reads

$$E(k_x, k_y) = -t[2 \cos(k_x) + 4 \cos(k_x/2) \cos(\sqrt{3}k_y/2)]. \quad (2)$$

This dispersion shows a logarithmic Van Hove singularity at $E=2t$, and at this energy value, the Fermi surface is hexagonal

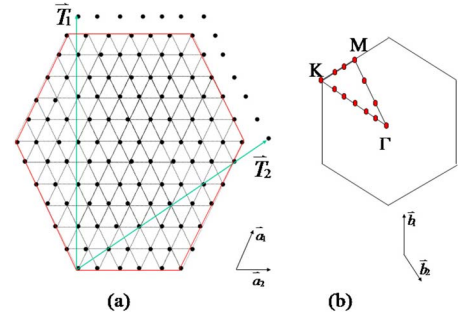


FIG. 1. (Color online) (a) Sketch of the triangular lattice. Here, \vec{a}_1, \vec{a}_2 are the primitive vectors of the underlying lattice. The real space lattice translational vectors are \vec{T}_1, \vec{T}_2 . The hexagon (red line) marked by the red lines defines the unit cell of the system. There are $2N$ sites in each diagonal. The case of $N=6$ is shown here. (b) First BZ of the triangular lattice. The red points represent the high symmetry points including Γ , M , and K points. \vec{b}_1, \vec{b}_2 are primitive vectors of the reciprocal lattice perpendicular to \vec{a}_1, \vec{a}_2 , which make the BZ 90° rotated to the real space lattice.

and the area is exactly $\frac{3}{4}$ of the whole BZ.³⁴ This dispersion implies that high DOS occurs when $E_F > 2t$ corresponding to electron filling above 1.5. This high DOS contributes to the strengthening of ferromagnetic spin fluctuation in this region.

In order to study the magnetic correlations on the triangular lattice, we calculate the spin susceptibility in the z direction at frequency $\omega=0$,

$$\chi(\mathbf{q}) = \int_0^\beta d\tau \sum_{i,j} e^{i\mathbf{q}\cdot(\mathbf{i}-\mathbf{j})} \langle \mathbf{m}_i(\tau) \cdot \mathbf{m}_j(0) \rangle, \quad (3)$$

where $m^\nu(\mathbf{i}, \tau) = e^{H\tau} m^\nu(\mathbf{i}, 0) e^{-H\tau}$ with $m_i \equiv c_{i\uparrow}^\dagger c_{i\uparrow} - c_{i\downarrow}^\dagger c_{i\downarrow}$.

III. RESULTS AND DISCUSSIONS

In the filling regions under investigation, the spin susceptibility behaviors are qualitatively the same. First, we present here the result at electron filling $\langle n \rangle = 1.75$. Figure 2 shows $\chi(q)$ versus q at different temperatures for $U=4|t|$ on a 108-site lattice. One can see that $\chi(q)$ has a broad peak around the Γ point of the BZ, indicating that the system exhibits a certain kind of ferromagnetic fluctuation. One can also see that the peak $\chi(q)$ at $\mathbf{q}=0$ does not grow rapidly with decreasing temperature. In the temperature range of $0.17|t| \leq T \leq 0.33|t|$, the growth of $\chi(q=0)$ seems to be slow. Figure 3 shows similar results for the case of $U=8|t|$. It is shown that the behavior at $U=8|t|$ is similar to the one at $U=4|t|$. At the same temperature, $\chi(q=0)$ at $U=8|t|$ is relatively larger than that at $U=4|t|$, suggesting that the on-site Coulomb interaction U tends to strengthen the ferromagnetic fluctuation. However, the numerical difficulty prevents further observation on temperature lower than $T=0.333|t|$, and there is no conclusive result about the low-temperature behavior of $\chi(q, U=8|t|)$. In Fig. 4, we show the results of $\chi(q)$ as a function of interaction strength U and β on three different lattices: 48 sites, 108 sites, and 147 sites. The data for dif-

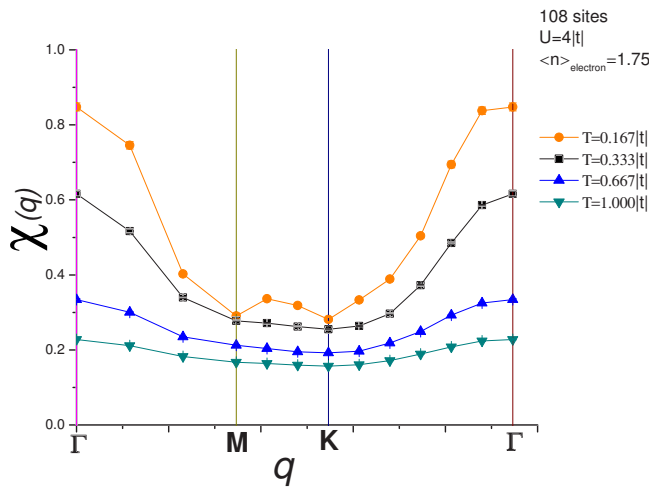


FIG. 2. (Color online) Magnetic susceptibility $\chi(\mathbf{q})$ versus the momentum \mathbf{q} at various temperatures down to $T=0.167|t|$ for $U=4|t|$ and the electron filling $\langle n \rangle = 1.75$. Data are shown along the path $\Gamma \rightarrow M \rightarrow K \rightarrow \Gamma$ in the hexagonal BZ.

ferent lattice sizes basically agree within statistical error. Since $\chi(q)$ obtained by summing up all lattice sites does not increase with the lattice size, we conclude that the ferromagnetic correlations in this system are short ranged. Figure 5 shows the behavior of $\chi(q)$ at different fillings for $U=4|t|$, and T is fixed at $0.167|t|$. Figure 6 shows $\chi(q=0)$ at different fillings and temperatures. It is clearly seen that the ferromagnetic fluctuation is strengthened when electron filling moves to the region with higher DOS in the noninteracting case, and $\chi(q=0)$ grows faster when one moves toward $\langle n \rangle = 1.5$. This indicates that the high DOS region favors the ferromagnetic fluctuation.

The occurrence of ferromagnetic ground state can also be inferred by comparing energies at different spin subspaces. In Table I, we show numerical results of the ground state energy obtained by the CPMC method. To simplify the CPMC simulations, we have used the hole picture for high

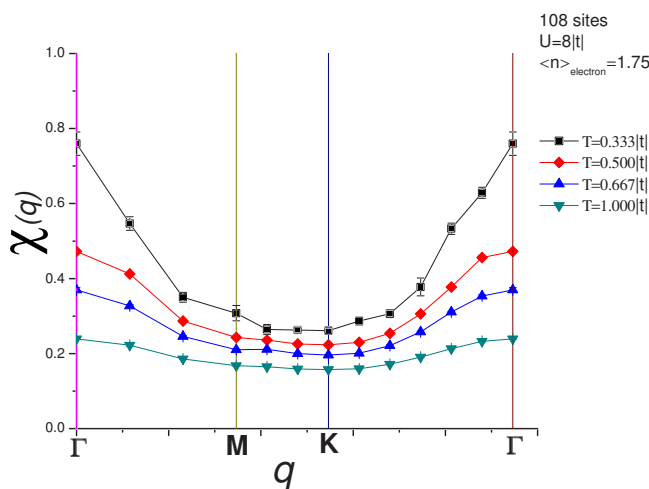


FIG. 3. (Color online) Magnetic susceptibility $\chi(\mathbf{q})$ versus the momentum \mathbf{q} at various temperatures down to $T=0.333|t|$ for $U=8|t|$. The filling is the same as the previous $U=4|t|$ case.

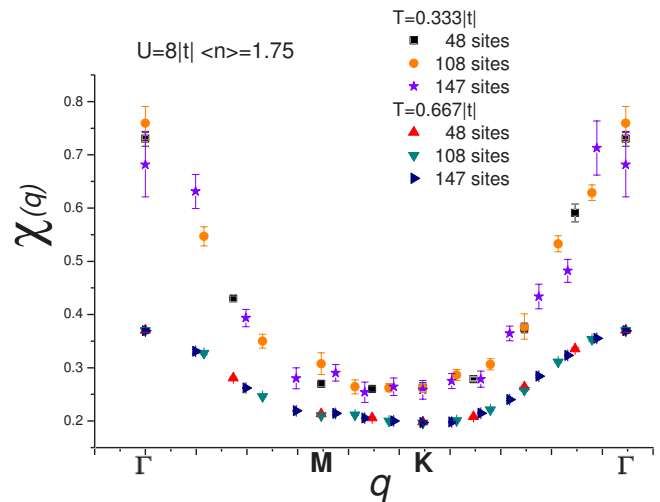


FIG. 4. (Color online) $\chi(\mathbf{q})$ on different lattices for $U=8|t|$ and $\langle n \rangle = 1.75$. Data at $T=0.667|t|$ and $T=0.333|t|$ are plotted.

fillings of electrons, i.e., describing the system with a negative t and hole filling $2 - \langle n \rangle$. We compare four cases on the 108-site lattice: (1) case 1, 13 holes with spin up and 1 hole with spin down versus 7 up and 7 down (total of 14 holes, corresponding to electron filling $\langle n \rangle_{\text{electron}} \approx 1.87$); (2) case 2, 19 holes with spin up and 7 holes with spin down versus 13 up and 13 down (total of 26 holes, corresponding to electron filling $\langle n \rangle_{\text{electron}} \approx 1.76$); (3) case 3, 20 electrons with spin up and 8 electrons with spin down versus 14 up and 14 down (total of 28 electrons, corresponding to electron filling $\langle n \rangle_{\text{electron}} \approx 0.26$); (4) case 4, 14 electrons with spin up and 2 electrons with spin down vs 8 up and 8 down (total of 16 electrons, corresponding to electron filling $\langle n \rangle_{\text{electron}} \approx 0.15$).

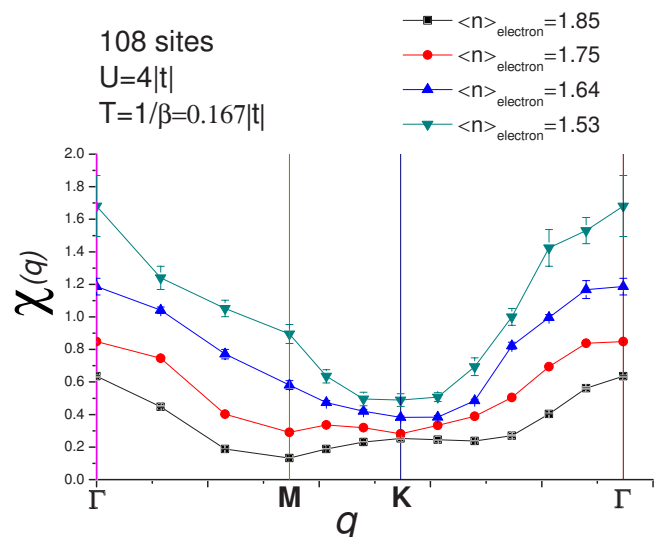


FIG. 5. (Color online) $\chi(\mathbf{q})$ versus \mathbf{q} at different fillings. The filling varies from $\langle n \rangle = 1.85$ to the value around the filling $\langle n \rangle = 1.5$ corresponding to the Van Hove singularity point of the noninteracting case. The data become more fluctuating when the filling is near $\langle n \rangle = 1.5$. The ferromagnetic fluctuation tends to be strengthened when filling decreases from a high value to near that corresponding to the Van Hove singularity.

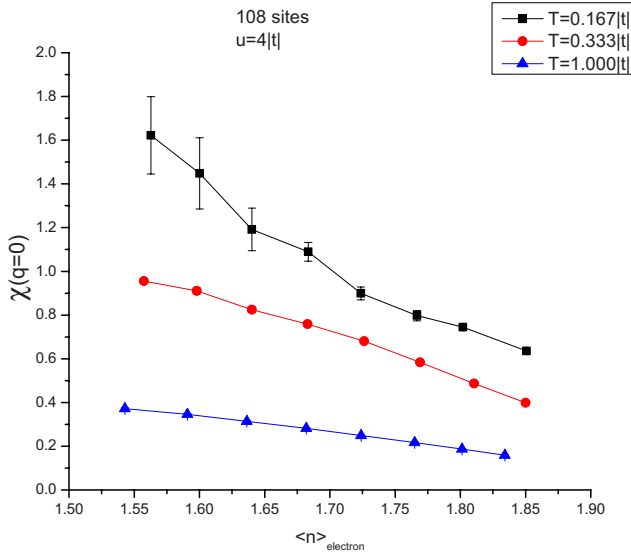


FIG. 6. (Color online) $\chi(\mathbf{q}=0)$ versus filling at $U=4|t|$. The filling varies from $\langle n \rangle = 1.85$ to the value around the filling $\langle n \rangle = 1.5$ corresponding to the Van Hove singularity point of the noninteracting case. The temperature varies from $T=1.000|t|$ to $T=0.167|t|$.

Table I and Fig. 7 show that as the Hubbard U is increased, the energy difference $\Delta = E_0^u - E_0^e$ between the paramagnetic ground state and the partially polarized ground state is reduced for most cases, suggesting that the ferromagnetic instability increases with increasing Coulomb interaction. In the figure, it is clearly shown that the energy difference is smaller for high fillings of electrons than that for low fillings of electrons. In particular, around the Van Hove sin-

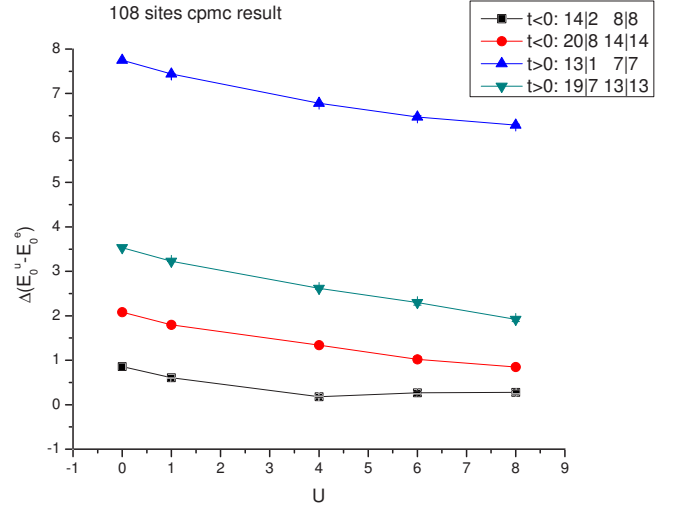


FIG. 7. (Color online) Ground state energy differences $\Delta = (E_0^u - E_0^e)$ between $S \neq 0$ and $S=0$ for different close shell cases.

gularity point, the energy levels get closer to each other compared to other regions, where we observe pronounced ferromagnetic fluctuations. These results give a very good example to quantitatively support the theoretical scenario mentioned above.

Our calculations also extend across the Van Hove singularity point to the $\langle n \rangle < 1.5$ region. The data become much more fluctuating and the peak of $\chi(q)$ seems to shift toward the M point. This may be caused by the competition between ferromagnetic and antiferromagnetic fluctuations. Since antiferromagnetic correlations are strong around the half-filling region,^{34,35} they may dominate the shape of $\chi(q)$ in a wide filling range up to near the Van Hove singularity point. We

TABLE I. Comparison of ground state energies for the same number of total particles in different spin subspaces: (1) spin up equal to spin down and (2) spin up unequal to spin down. We show the results at four different fillings. $U=0$ case corresponds to the noninteracting case, $t > 0$ implies that the particle stands for electron, and $t < 0$ for hole. Here, $\Delta = (E_0^u - E_0^e)$ is the energy difference between two spin subspaces. E_0^u corresponds to the system with unequal numbers of spin up and spin down particles, while E_0^e corresponds to the system with equal numbers of spin up and spin down particles.

U	0	$1 t $	$4 t $	$6 t $	$8 t $
$t < 0$					
16 particles (14 \uparrow 2 \downarrow)	-43.745	48.465(1)	325.130(8)	509.84(1)	694.29(2)
16 particles (8 \uparrow 8 \downarrow)	-44.603	47.859(2)	324.950(8)	509.57 (2)	694.01(2)
$\Delta = (E_0^u - E_0^e)$	0.857	0.606(3)	0.18(2)	0.27(3)	0.28(4)
28 particles (20 \uparrow 8 \downarrow)	-73.407	7.810(4)	250.30(2)	411.45(2)	572.10(2)
28 particles (14 \uparrow 14 \downarrow)	-75.490	6.013(4)	248.96(2)	410.43(4)	571.25(2)
$\Delta = (E_0^u - E_0^e)$	2.084	1.797(8)	1.34(4)	1.02(6)	0.85(4)
$t > 0$					
14 particles (13 \uparrow 1 \downarrow)	-67.745	-67.635(1)	-67.395(5)	-67.28(1)	-67.142(7)
14 particles (7 \uparrow 7 \downarrow)	-75.490	-75.075(1)	-74.172(6)	-73.75(2)	-73.43(1)
$\Delta = (E_0^u - E_0^e)$	7.75	7.440(2)	6.78(1)	6.47(3)	6.29(2)
26 particles (19 \uparrow 7 \downarrow)	-119.959	-118.819(2)	-116.24(1)	-115.06(3)	-114.16(2)
26 particles (13 \uparrow 13 \downarrow)	-123.490	-122.044(3)	-118.864(7)	-117.36(3)	-116.08(3)
$\Delta = (E_0^u - E_0^e)$	3.531	3.225(5)	2.62(2)	2.30(6)	1.92(5)

argue that in this region, although the ferromagnetic fluctuation cannot overwhelm the antiferromagnetic fluctuation, the competition between them will suppress antiferromagnetic correlations and the peak of $\chi(\mathbf{q})$ moves toward the M point, between K point and Γ point. These results agree with previous studies using different methods. For example, the mean field study³⁴ showed that the ferromagnetic correlation is more favorable near the Van Hove singularity point than other filling regions and competes with the antiferromagnetic correlation near the half-filling region. The perturbation study²⁴ showed that the change of the Van Hove singularity point by adjusting the next-nearest-neighbor hopping integral properly,²³ can lead to the situation where the bare spin susceptibility shows ferromagnetic correlation. So, we can see from the quantum Monte Carlo calculations that the high DOS near the Van Hove singularity point is crucially important to the enhancement of the ferromagnetic fluctuation.

In the same fillings discussed above, we also study the behaviors of pairing correlations in different channels. The imaginary-time pair-field operator is defined as^{36,37}

$$\Delta_\alpha(\tau) = \frac{1}{\sqrt{N_s}} \sum_k f_\alpha(k) c_{k\uparrow}(\tau) c_{-k\downarrow}(\tau). \quad (4)$$

By the Fourier transform, the site-dependent pair-field operator is introduced,

$$\begin{aligned} \Delta_\alpha(\tau) &= \frac{1}{\sqrt{N_s}} \sum_i \Delta_\alpha(i, \tau) \\ &= \frac{1}{\sqrt{N_s}} \sum_{i,l} f_\alpha(l) \langle c_{i\uparrow}(\tau) c_{i+l\downarrow}(\tau) \pm c_{i+l\uparrow}(\tau) c_{i\downarrow}(\tau) \rangle, \end{aligned} \quad (5)$$

where the sum runs over lattice sites l and neighboring sites i , and $f_\alpha(l)$ is the site-dependent form factor of electron pairs. Simple averages of pair-field operators vanish identically in a finite-sized system, so we turn to correlation functions. At finite temperature, the time-dependent pairing susceptibility is a useful probe for pairing interaction.³⁷⁻³⁹ We define the uniform and zero-frequency ($\omega=0$) pairing susceptibility,

$$P_\alpha = \frac{1}{N_s} \sum_{i,j} \int_0^\beta d\tau \langle \Delta_\alpha^+(i, \tau) \Delta(j, 0) \rangle. \quad (6)$$

Considering the symmetry of the triangular lattice, possible form factors include the following six types:

$$f_s(l) = \frac{1}{\sqrt{6}} [\delta_{l,\bar{a}_1} + \delta_{l,-\bar{a}_1} + \delta_{l,\bar{a}_2} + \delta_{l,-\bar{a}_2} + \delta_{l,\bar{a}_1+\bar{a}_2} + \delta_{l,-\bar{a}_1-\bar{a}_2}],$$

$$f_{d_{xy}}(l) = \frac{1}{2\sqrt{3}} [\delta_{l,\bar{a}_2} + \delta_{l,-\bar{a}_2} - \delta_{l,\bar{a}_1,\bar{a}_2} - \delta_{l,-\bar{a}_1-\bar{a}_2}],$$

$$\begin{aligned} f_{d_{x^2-y^2}}(l) &= \frac{1}{2} [2\delta_{l,\bar{a}_1} + 2\delta_{l,-\bar{a}_1} - \delta_{l,\bar{a}_2} - \delta_{l,-\bar{a}_2} - \delta_{l,\bar{a}_1+\bar{a}_2} \\ &\quad - \delta_{l,-\bar{a}_1-\bar{a}_2}], \end{aligned}$$

$$f_f(l) = \frac{1}{2\sqrt{3}} [\delta_{l,\bar{a}_1} - \delta_{l,-\bar{a}_1} + \delta_{l,\bar{a}_2} - \delta_{l,-\bar{a}_2} + \delta_{l,\bar{a}_1+\bar{a}_2} - \delta_{l,-\bar{a}_1-\bar{a}_2}],$$

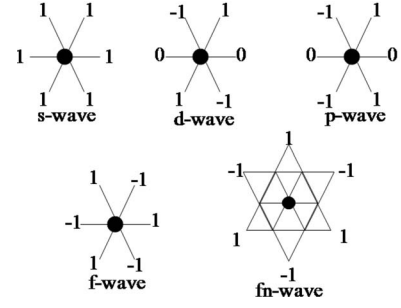


FIG. 8. Site-dependent form factors for s wave, d wave, p wave, f wave, and fn wave on the triangular lattice.

$$f_{p_x}(l) = \frac{1}{2} [\delta_{l,\bar{a}_2} - \delta_{l,-\bar{a}_2} + \delta_{l,\bar{a}_1+\bar{a}_2} - \delta_{l,-\bar{a}_1-\bar{a}_2}],$$

$$\begin{aligned} f_{p_y}(l) &= \frac{1}{\sqrt{6}} [-2\delta_{l,\bar{a}_1} + 2\delta_{l,-\bar{a}_1} + \delta_{l,\bar{a}_2} - \delta_{l,-\bar{a}_2} - \delta_{l,\bar{a}_1+\bar{a}_2} \\ &\quad + \delta_{l,-\bar{a}_1-\bar{a}_2}]. \end{aligned}$$

The former three are singlet pairing and the latter three are triplet. Assuming that the triangular lattice is isotropic, the $d_{x^2-y^2}$ wave, d_{xy} wave, p_x wave, and p_y wave are degenerate. We denote them as the d wave and p wave, as shown in Fig. 8. The extended s wave and the f wave with next nearest neighbors are denoted as s wave and fn wave, respectively.

The behaviors of all kinds of pairing susceptibility do not change qualitatively in the major part of the filling region we studied. We show two typical fillings, $\langle n \rangle = 1.60$ and $\langle n \rangle = 1.85$. For the case of $\langle n \rangle = 1.60$, as shown in Fig. 9, one can see that up to the temperature $T = 0.167|t|$, all kinds of pairing susceptibility tend to increase, and the f wave increases fastest. However, it is not clear whether the susceptibilities keep growing at lower temperatures since the sign problem pre-

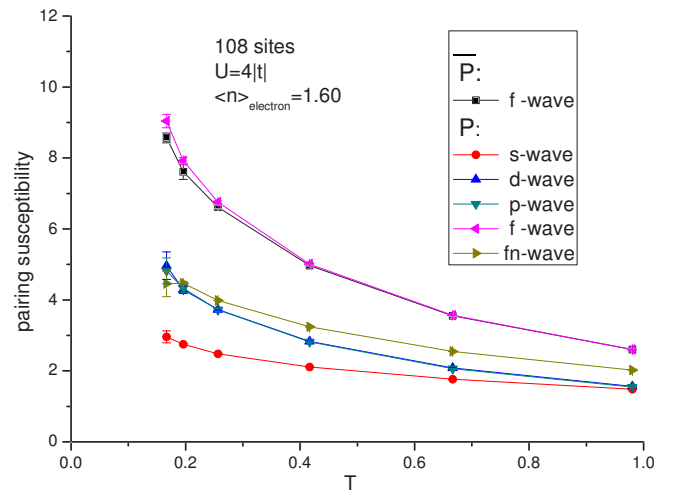


FIG. 9. (Color online) Pairing susceptibility as a function of temperature for different pairing symmetries at $U=4|t|$ and $\langle n \rangle = 1.60$.

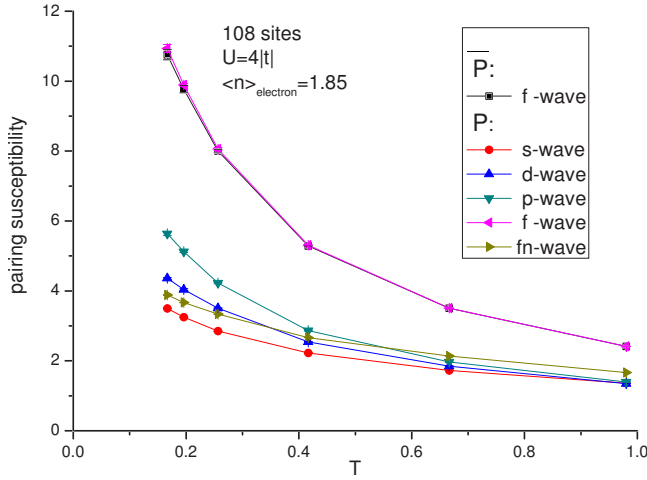


FIG. 10. (Color online) Pairing susceptibility as a function of temperature for different pairing symmetries at $U=4|t|$ and $\langle n \rangle = 1.85$.

vents simulations in the low-temperature regime. Figure 10 displays similar results for the filling, $\langle n \rangle = 1.85$. It is clearly seen that the spin-triplet p -wave and f -wave pairing susceptibilities keep growing; particularly, the f wave still grows fastest, while the other waves (s wave, d wave, and fn wave) seem to saturate. Notice that these kinds of pairing susceptibilities contain the single-particle contribution, i.e., $\langle c_{i\uparrow}^+ c_{j\uparrow} \rangle \langle c_{i+l\downarrow}^+ c_{j+l'\downarrow} \rangle$, etc., which does not include the effects of particle-particle interaction. In order to extract the effective pairing interactions in different pairing channels, we also evaluate the single-particle contribution $\bar{P}_\alpha(i, j)$,^{32,40} by replacing $\langle c_{i\uparrow}^+ c_{j\uparrow} \rangle \langle c_{i+l\downarrow}^+ c_{j+l'\downarrow} \rangle$ with $\langle c_{i\uparrow}^+ c_{j\uparrow} \rangle \langle c_{i+l\downarrow}^+ c_{j+l'\downarrow} \rangle$ in Eq. (5). In Figs. 9 and 10, we plot \bar{P}_f for comparison. It is apparent that \bar{P}_f shows a very similar temperature dependence as P_f . The effective pairing interaction, which can be estimated by the difference between P_f and \bar{P}_f , is shown to be small. We also observe that the effective pairing interaction is stronger for $\langle n \rangle = 1.60$ than for $\langle n \rangle = 1.85$, demonstrating that increasing ferromagnetic spin fluctuations when approaching the Van Hove singularity contributes more to the f -wave pairing.

Although our results show that the ferromagnetic fluctuations enhance the f -wave pairing susceptibility more than other pairing susceptibilities, it is not clear how this triplet pairing correlation behaves in the lower temperature regime $T < 0.1|t|$. However, it is interesting to see that the f -wave

pairing correlation dominates in a wide region where the system shows ferromagnetic fluctuation, which agrees with the perturbation studies on a relevant case.²⁴ The perturbation results suggested that a spin-triplet f -wave pairing is the most stable in a wide parameter range, and by tuning the position of the Van Hove singularity such as adding the next-nearest-neighbor hopping integral, the spin susceptibility shows a broad peak around Γ point, and these conditions stabilize the f -wave pairing. Combining symmetry-based considerations with inputs from available experimental results also shows the possibility of spin-triplet pairing in the filling region near the Van Hove singularity point.²⁹ Assuming that there exists an f -wave superconductivity at low temperatures, our numerical results suggest that the transition temperature would be very low due to the very weak pairing interaction. This is in good agreement with the perturbation calculation²⁴ and the high-temperature expansions,³² where the f -wave instability was found to be weak in a wide filling region.

IV. SUMMARY

To summarize, we have studied the spin susceptibility $\chi(q)$, the ground state energy, and the pairing susceptibility of the single-band Hubbard model on the triangular lattice. We found that in the filling region above $\langle n \rangle = 1.5$ (corresponding to the filling at the Van Hove singularity point), the system shows a weak short-ranged ferromagnetic correlation, which is slightly strengthened by the Coulomb interaction. We also saw that around the ferromagnetic region, the f -wave triplet pairing grows faster than other pairing channels, but the effective pairing interaction is very weak, which is consistent with the previous work⁴¹ done by Kumar and Shastry.

ACKNOWLEDGMENTS

The authors thank Wen-Long You, Shi-Jian Gu, Jin An, and Jiang-Long Wang for useful discussions. H.-Q.L. and S.-Q.S. thank Frank Ng and Albert Lau at the ITSC of CUHK, where a large amount of the numerical work presented in this paper was accomplished. This work is supported by HKSAR RGC Project No. CUHK 401806. Z.-B.H. is supported by NSFC Grants No. 10574040 and No. 10674043. Part of the work was carried out while H.-Q.L. was visiting KITPC and he greatly appreciates its hospitality.

¹G. Baskaran, Phys. Rev. Lett. **91**, 097003 (2003).
²W. Koshibae and S. Maekawa, Phys. Rev. Lett. **91**, 257003 (2003).
³K. Takada, H. Sakurai, E. Takayama-Muromachi, F. Izumi, R. A. Dilanian, and T. Sasaki, Nature (London) **422**, 53 (2003).
⁴N. Tajima, T. Imakubo, R. Kato, Y. Nishio, and K. Kajita, J. Phys. Soc. Jpn. **72**, 1014 (2003).
⁵M. C. Gutzwiller, Phys. Rev. Lett. **10**, 159 (1963).

⁶J. Hubbard, Proc. R. Soc. London, Ser. A **276**, 238 (1963).
⁷J. Kanamori, Prog. Theor. Phys. **30**, 275 (1963).
⁸Y. Nagaoka, Phys. Rev. **147**, 392 (1966).
⁹D. J. Thouless, Proc. Phys. Soc. London **86**, 893 (1965).
¹⁰T. Hanisch, G. S. Uhrig, and E. Müller-Hartmann, Phys. Rev. B **56**, 13960 (1997).
¹¹H. Tasaki, Phys. Rev. B **40**, 9192 (1989).
¹²E. H. Lieb, Phys. Rev. Lett. **62**, 1201 (1989).

- ¹³A. Mielke, Phys. Lett. A **174**, 443 (1993).
¹⁴A. Mielke, Phys. Rev. Lett. **82**, 4312 (1999).
¹⁵H. Tasaki, Phys. Rev. Lett. **69**, 1608 (1992); A. Mielke and H. Tasaki, Commun. Math. Phys. **158**, 341 (1993).
¹⁶H. Tasaki, Phys. Rev. Lett. **75**, 4678 (1995).
¹⁷H. Tasaki, Phys. Rev. Lett. **73**, 1158 (1994).
¹⁸R. Hlubina, S. Sorella, and F. Guinea, Phys. Rev. Lett. **78**, 1343 (1997).
¹⁹S. Daul and R. M. Noack, Phys. Rev. B **58**, 2635 (1998).
²⁰T. Wegner, M. Potthoff, and W. Nolting, Phys. Rev. B **57**, 6211 (1998).
²¹Liliana Arrachea, Phys. Rev. B **62**, 10033 (2000).
²²K. Takashi and M. Ogata, J. Phys. Soc. Jpn. **72**, 2437 (2003).
²³H. Q. Lin and J. E. Hirsch, Phys. Rev. B **35**, 3359 (1987).
²⁴H. Ikeda, Y. Nisikawa, and K. Yamada, J. Phys. Soc. Jpn. **73**, 17 (2004).
²⁵Y. Nisikawa and K. Yamada, J. Phys. Soc. Jpn. **71**, 2629 (2002).
²⁶C. Honerkamp, Phys. Rev. B **68**, 104510 (2003).
²⁷K. Kuroki and R. Arita, Phys. Rev. B **63**, 174507 (2001).
²⁸K. Kuroki, Y. Tanaka, and R. Arita, Phys. Rev. Lett. **93**, 077001 (2004).
²⁹A. Tanaka and X. Hu, Phys. Rev. Lett. **91**, 257006 (2003).
³⁰Q. H. Wang, D. H. Lee, and P. A. Lee, Phys. Rev. B **69**, 092504 (2004).
³¹T. Watanabe, H. Yokoyama, Y. Tanaka, J. Inoue, and M. Ogata, J. Phys. Soc. Jpn. **73**, 3404 (2004).
³²T. Koretsune and M. Ogata, Phys. Rev. B **72**, 134513 (2005).
³³R. Blankenbecler, D. J. Scalapino, and R. L. Sugar, Phys. Rev. D **24**, 2278 (1981).
³⁴Thoralf Hanisch, Burkhard Kleine, Afra Ritzl, and Erwin Muller-Hartmann, Ann. Phys. (N.Y.) **507**, 303 (1995).
³⁵N. Bulut, W. Koshibae, and S. Maekawa, Phys. Rev. Lett. **95**, 037001 (2005).
³⁶D. R. Tilley and J. Tilley, *Superfluidity and Superconductivity*, 3rd ed. (Adam Hilger, Bristol and New York, 1990).
³⁷J. E. Hirsch and H. Q. Lin, Phys. Rev. B **37**, 5070 (1988); H. Q. Lin, J. E. Hirsch, and D. J. Scalapino, *ibid.* **37**, 7359 (1988).
³⁸R. R. dos Santos, Phys. Rev. B **39**, 7259 (1989).
³⁹H. Q. Lin and J. E. Hirsch, Phys. Rev. B **52**, 16155 (1995).
⁴⁰S. R. White, D. J. Scalapino, R. L. Sugar, E. Y. Loh, J. E. Gubernatis, and R. T. Scalettar, Phys. Rev. B **40**, 506 (1989).
⁴¹B. Kumar and B. S. Shastry, Phys. Rev. B **68**, 104508 (2003).